Published in final edited form as:

Macromolecules. 2016 July 26; 49(14): 5076–5083. doi:10.1021/acs.macromol.6b01048.

Surface-Anchored Poly(*N*-isopropylacrylamide) Orthogonal Gradient Networks

C. K. Pandiyarajan[†], **Michael Rubinstein**[*,‡], and **Jan Genzer**[*,†]

[†]Department of Chemical & Biomolecular Engineering, North Carolina State University, Raleigh, North Carolina 27695-7905, United States

[‡]Department of Chemistry, University of North Carolina, Chapel Hill, North Carolina 27599-3290, United States

Abstract

We present a versatile synthetic route leading toward generating surface-attached polyacrylamide gels, in which the cross-link density varies continuously and gradually across the substrate in two orthogonal directions. We employ free radical polymerization to synthesize random copolymers comprising ~5% of photoactive methacrylyloxybenzophenone (MABP), ~5% of thermally active styrene sulfonyl azide (SSAz), and ~90% of *N*-isopropylacrylamide (NIPAAm) units. The presence of MABP and SSAz in the copolymer facilitates control over the cross-link density of the gel in an orthogonal manner using photoactivated and thermally activated cross-linking chemistries, respectively. Spectroscopic ellipsometry is employed to determine the degree of swelling of the gel in water and methanol as a function of position on the substrate. Network swelling varies continuously and gradually across the substrate and is high in regions of low gel fractions and low in regions of high gel fractions.

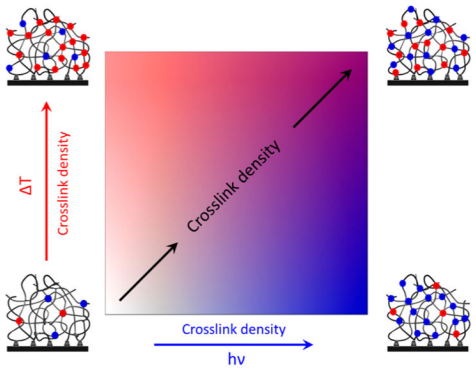

[*]**Corresponding Authors**, mr@unc.edu (M.R.)., jgenzer@ncsu.edu (J.G.). .

Supporting Information

The Supporting Information is available free of charge on the ACS Publications website at DOI: 10.1021/acs.macro-mol.6b01048. Experimental details; Figures S1–S7 and Table S1 (PDF)

Notes

The authors declare no competing financial interest.

During the past five decades immense exertion has been made in generating surfaces presenting physicochemical gradients[1] due to their inevitable usage in many fields and applications, including, tissue engineering,[2] drug delivery,[3] biosensors,[4] or microfluidics.[5] Surface gradients exemplify continuous and gradual variation of at least one physicochemical property (e.g., wettability, modulus, topography, density of grafts) of the coating layer. One area that benefits greatly from gradient structures is biology, where gradient material motifs are present naturally or can be fabricated by synthetic routes. For example, tendons, fibrous tissues found in our bodies, illustrate naturally occurring gradient materials; they exhibit a continuous change in modulus, which assist them to achieve efficient connectivity between soft muscle tissues and hard bones.[6,7] The development of synthetic gradients by invoking a simple chemical or physical approach facilitates systematic interrogation of the material on biological behavior while creating opportunities to study and model specific dynamic phenomena such as direct movement of water drops[8,9] and bacteria[10] or cell migration and differentiation.[6,11,12]

Numerous research groups described a broad spectrum of soft matter gradients based on surface-grafted polymer brushes.[1,13–15] Such surface-bound gradients are comprehended by functionality,[15–18] dimensionality,[19,20] directionality,[21,22] length scale,[23,24] and temporal dependency.[13,25,26] Specifically, functional gradients featuring various soft material building blocks enable systematic screening of interactions between biological macromolecules, i.e., proteins and platelets, with various supports that are vital in the development of blood compatible coatings for medical devices, e.g., ventricular assist devices (VAD).[27,28] A variety of diverse assembly methods[1,15] has been introduced by many researchers to fabricate surface-bound gradient coatings, including gas or liquid phase diffusion of self-assembling organosilanes, gel-based diffusion of alkanethiols on gold surfaces, diffusion in microfluidic channels, spatially localized corona discharge treatment of polymer surfaces, plasma-discharge methods, and in-plane electric field gradients to spatially desorb alkanethiols or electrodeposit metals or post-polymerization treatments.[1] While many functional substrates feature density gradient assemblies of small molecule modifiers, the low thickness of such systems often compromises the stability and broad application of such materials. Alternatively, assemblies of long chain molecules offer substantially thicker films extending to variation of surface concentrations of functional moieties as described in recent reviews.[13,15]

Herein, we report on a simple and versatile synthetic route to generate stable surface-tethered gradient polymer network coatings with continuous and gradual variation in cross-link density of the network. By employing two chemical functionalities that can be activated orthogonally by using two different external triggers, complex structures can be formed on a single substrate that feature gradual variation of the modulus in an orthogonal fashion (cf. Figure 1). To this end, we employ free radical polymerization to synthesize random copolymers comprising ~5% of photoactive methacrylyloxybenzophenone (MABP), ~5% of thermally active styrene sulfonyl azide (SSAz), and ~90% of *N*-isopropylacrylamide (NIPAAm) units. The number-average molecular weight and polydispersity index of the copolymer are 339 kDa and 2.5, respectively. The numbers of the MABP and SSAz units in the copolymer are ~89 and ~111, respectively. Experimental details pertaining to polymer synthesis and characterization are provided in the Supporting Information. Cross-linking can

thus be accomplished by (1) activating the MABP units with UV light at the wavelength of 254 or 364 nm or/and (2) annealing at temperatures >140 °C, a process that activates the SSAz sites. Taking advantage of the orthogonality of the cross-linkling reactions, we fabricate gradients in gel density propagating in two perpendicular directions on a single specimen by gradually varying the temperature and/or the UV dosage in two orthogonal directions. We use variable angle spectroscopic ellipsometry (VASE) to measure the dry film thickness before cross-linking (d_{film}) and after cross-linking followed by solvent extraction (d_0). The ratio d_0/d_{film} defines the gel fraction of the network. Similarly, the degree of swelling (i.e., swelling factor) of these network is the ratio of the gel film thickness in the presence of solvent (d_S) and dry gel film thickness (d_0) and is a function of the position on the sample. Gel regions featuring low cross-link density (either low UV dosage or low temperature) exhibit the highest degree of swelling. In contrast, positions on the sample containing highly cross-linked gels (high temperature or high UV dosage) swell to a lesser degree.

The surface-bound orthogonal gradient networks were generated through photo and thermal cross-linking of poly(NIPAAm$_{0.90}$-*co*-SSAz$_{0.05}$-*co*-MABP$_{0.05}$) films in two orthogonal directions as depicted in Figure 1a; the subscripts denote the approximate mole fractions of each unit in the copolymer. The SSAz and MABP cross-linkers were synthesized by employing a process similar to that described elsewhere.[28,30] The poly(NIPAAm$_{0.90}$-*co*-SSAz$_{0.05}$-*co*-MABP$_{0.05}$) copolymer was synthesized via free-radical polymerization (cf. Figure S1 in Supporting Information) initiated by AIBN. To enable the surface adhesion, all substrates were first covered with a thin layer of 4-[3-(triethoxysilyl)propyloxy]benzophenone (TESPBP, thickness 3–6 nm) prior to the polymer deposition.[28]

A solution of poly(NIPAAm$_{0.90}$-*co*-SSAz$_{0.05}$-*co*-MABP$_{0.05}$) in 1-butanol was spun-cast on a TESPBP-modified wafer. First, photo-cross-linking was performed by anchoring wafer to the dip-coater, which moved the sample under UV light (λ = 360 nm) at a speed of 10 mm/min for about 4 min with a constant dosage of 5.5 mW/cm^2. Upon illumination with UV light, benzophenone-based units present in the copolymer as well as in the silane layer got photoactivated and promoted simultaneous cross-linking of polymer chains in the copolymer and covalent attachment of the gel to the substrate. After photo-cross-linking, the sample was placed on a gradient heating stage, where the cross-linking was triggered solely by varying the temperature. Any polymeric material that was not a part of the network, i.e., unreacted chains or/and larger isolated macromolecular clusters formed by reacting several polymers but not connected to the network, was removed by solvent extraction. A complete fabrication process is depicted in Figure 1b.

The mechanisms of the two cross-linking reactions were investigated by Pandiyarajan et al.[28] and Schuh et al.[30] Concisely, benzophenone (BP) containing units absorb UV light, which results in a n–π^* or π–π^* transitions of carbonyl groups depending on the wavelength of the light (UV light, 360 nm, n–π^*).[31] Consequently, the biradicaloid triplets, i.e., two independent radicals on carbonyl group, are formed, which can potentially abstract proton from any adjacent C–H group, resulting two carbon-based radicals. Upon recombination those radicals generate a covalent bond (cf. Figure 1c). The recombination

reaction involving BP present in the surface-anchored monolayers attaches the polymer to the substrate. In contrast, UV activation of MABP results in the formation of intramolecular cross-links and ultimately gels.[30–34] The thermal cross-linker (SSAz) comprising a thermally active sulfonyl azide group releases nitrogen gas upon heating and forms nitrene, as shown in Figure 1d. The resultant nitrene either reacts with the C–H bond of the neighboring polymer chain via insertion reaction or abstracts the proton from the adjacent C–H bond followed by recombination yielding a bond. These bonds initially do not lead to the gel, as a certain number of bonds (~one intermolecular cross-link per chain) has to be formed first.[30] An attractive feature of this system is that is can be employed on many different surfaces, for instance, polystyrene (PS) or poly(methyl methacrylate) (PMMA) supports (*vide infra*).

In the process of preparing gradient networks, it is important to identify and optimize the cross-linking conditions, which lead to gel formation. Figure 2a depicts the gel fraction of photo (blue symbols) and thermal (red symbols) cross-linking process. UV-based reaction is relatively fast; even after 30 s of irradiation, the reaction yields ~60% of gel and increases to ~90% after ~4 min of UV treatment. Because extensive illumination with UV light can potentially damage the polymer film,[35] in all our experiments we keep the photo-cross-linking reaction to run up to 4 min with the dosage of 5.5 mW/cm^2. In related experiments, which will be reported separately, we prepared gels by exposing films of poly(NIPAAm$_{0.95}$-*co*-MABP$_{0.05}$), i.e., without the thermal cross-linker, to dosages ranging from 5.5 to 30 mW/cm^2. As expected, the rate of cross-linking increased with increasing UV dosage. We also investigated the influence of initial film thickness on gel content by preparing films with different initial layer thickness as indicated in Figure 2b. There were no significant differences in the gel content of the films ranging from 5 to 50 nm in initial thickness. A slight decrease in gel fraction was observed for thicker films irradiated with a dosage of 5.5 mW/cm^2. This may be due to UV absorption in the film, leading to a slight increase of the sol fraction, for films whose initial thicknesses are larger than ~100 nm.

The gel fraction in thermally activated cross-linking process was also studied (cf. Figure 2a, red symbols). The temperature required for the cross-linking process was established by heating a series of polymer layers at various temperatures for 300 min. The maximum gel content (~90%) was achieved after annealing the samples at 140 °C for 300 min. This is evidenced by Fourier transform infrared spectroscopy (FTIR) experiments, where the deposited polymer films were heated at 140 °C for different time intervals (cf. Figure 2a, inset), and the IR spectra were recorded. A progressive attenuation in the absorbance of azide functionality (N═N═N) at 2130 cm^{-1} reveals that the azide groups are consumed progressively during the course of the reaction. A near disappearance of azide peak after 300 min suggests that almost all azide motifs have been converted into sulfamides. This is in agreement with the gel contents obtained from thickness measurements, which reveal a gel content of 95% at 300 min of annealing. Further increase in gel content may be achieved by increasing the concentration of the cross-linking groups along the polymer and/or increasing the annealing time. Under the conditions studied, the thermal cross-linking was found to be ~16.7 times slower than the UV-activated process with the dosage of 5.5 mW/cm^2. In a separate publication we will discuss the kinetics of cross-linking in macromolecules that possess random distribution of cross-link centers and test the model against experiments in

which poly(NIPAAm$_{1-y}$-*co*-MABP$_y$), where y ranges from 0.03 to 0.10, was exposed to UV light with dosages ranging from 5.5 to 30 mW/cm^2.[36]

After optimizing the cross-linking conditions, surface-bound orthogonal gradient networks were generated using two triggers that featured UV/UV cross-linking, thermal/thermal cross-linking, and UV/thermal cross-linking in orthogonal directions. The gel fraction as a function of position on the specimen was evaluated using VASE. Each sample was divided into 3 × 3 squares (matrices), each with a dimension of 1 cm × 1 cm. On each square, 2–3 reflectivity scans were performed and modeled in accordance with Fresnel formalisms, and the average thickness was taken into account (cf. Figure S2).

In Figure 3a, we plot the gel content in a UV orthogonally cross-linked sample (i.e., MABP/MABP). The cross-linking reaction through MABP is very fast; after only 30 s the reaction yields ~60% of gel content. The presence of second independent trigger, i.e., SSAz, allows us to tune cross-link density in an orthogonal direction by thermally activating only the SSAz units (cf. Figure 3b) (i.e., SSAz/SSAz). For example, if the sample is cross-linked thermally twice from A → C or 1 → 3, a continuous gel gradient develops when we visualize the sample diagonally from A1 → C3; the variation gel fraction is small in the A3 → C3 or C1 → C3 directions. This is because before the application of the second cross-linking trigger the sol fraction in the existing gel is already relatively small. Next we consider orthogonal samples prepared by employing the UV- and thermally induced cross-linking as two independent triggers, i.e., A → C (e.g., UV) and 1 → 3 (e.g., thermal), to generate surface-attached orthogonal gradient networks.

Figure 3c depicts a specimen featuring a gradient in gel content that was prepared by UV cross-linking (Ax → Bx → Cx) followed by thermal cross-linking (x1 → x2 → x3) (i.e., MABP/SSAz). The film thickness increases from A1 → A2 → A3 or from A1 → B1 → C1 and decreases from C3 → C2 → C1 or from C3 → B3 → A3. The positions on the samples that were strongly cross-linked either thermally (A3, B3, C3) or via UV-light (C1, C2, C3) were found to be thicker than the rest of the regions that reacted to a lesser degree by either of the cross-linking processes. The largest thickness increase was observed when examining the specimens diagonally from A1 → B2 → C3. The change in the film thickness depends strongly on the extent at which the gel is reacted through UV and/or thermal cross-linking reactions. This is evidenced by examining the reflectivity scans obtained from spectroscopic ellipsometry (cf. Figure S3), where the maximum reflectivity (R_{max}) of a scan is probed. For example, the R_{max} of C3 is observed at a longer wavelength ~680 nm, while A1 exhibits ~590 nm. Upon modeling these scans, the film thickness of C3 is found to be larger ($d_{A1} \approx 142$ nm) than that of A1 ($d_{C3} \approx 122$ nm). This is expected because C3 is strongly cross-linked by both photo and thermal processes, whereas A1 is incompletely reacted by either of the two cross-linking processes. A similar tendency is witnessed (thickness increases) in going from A1 → A3 or B1 → B3 or C1 → C3. The VASE reflectivity scans can thus be employed as an efficient tool to probe the surface profile of a gradient coating. We also prepared a specimen, in which the order of the UV and thermal cross-linking triggers was reversed; i.e., the polymer was first cross-linked thermally and then via UV (both in the same gradient fashion as described earlier). The gel content

was found to be similar to the data reported in Figure 3c. This confirmed that the sequence of the cross-linking events does not influence the gel content in the sample (cf. Figure S4).

We extended the aforementioned strategy on a polymeric substrate, typically 10–15 nm thick PMMA layer deposited on top of a silica wafer. The orthogonal gradient network was generated in the same way as that on benzophenone silane covered wafer. The results are displayed in Figure 3d, where the gradient behavior is clearly inferred across the samples. The observed trends are in agreement with the results presented in Figure 3c. These results demonstrate successfully that our strategy is robust and can be adopted to fabricate a gradient coverage on any polymeric surfaces as long as the polymer precursor possesses C–H backbone or side chains required for cross-linking. The presence of two mutually orthogonal cross-linking chemistries (i.e., photo vs thermal) enables us to tune the cross-linking density of the gel independently in two different directions with high accuracy.

We examined swelling of gradient gels using a liquid cell attached to VASE. The reflectivity scans were recorded on each square of the gradient coatings and the optical components of the swollen gels were derived from modeling the data based on Fresnel formalism (cf. Figure 4 and Table S1 in Supporting Information). We define a swelling factor (α) of the gel as the ratio of the thicknesses of the swollen film (d_s) and the dry film after extraction of sol fraction (d_o); ϕ_s is the polymer volume fraction:[28]

$$\alpha = \frac{d_s}{d_o} = \frac{1}{\phi_s} \quad (1)$$

We examined gel swelling under humid air environment ranging from ~13 to ~98% of relative humidity, RH (cf. Figure S5). Up until RH 65–70% the gel swelling was relatively small, illustrating that the film thickness measured at ambient condition (RH ~ 45–50%, T ~ 25 °C) can be considered reasonably as a being a dry film having thickness d_o. However, the gels swell to ~1.12 ± 0.01 at high RH due to the sufficient amount of water vapor present in the air (water content ~2.5% at 98% RH).

In Figure 4 we plot the swelling factors as a function of gel content for all three gradients i.e., MABP/MABP, SSAz/SSAz, and MABP/SSAz gels swollen in methanol and water (MABP/SSAz). Swelling decreases with increasing gel content indicating that higher gel content corresponds to networks with a higher cross-link density (i.e., degree of cross-linking). For instance, A1 with lower cross-link density (i.e., weakly cross-linked) swells strongly in methanol. Swelling decreases from A → B → C or 1 → 2 → 3 due to the increase in the cross-link density of the gel. This phenomenon is governed by the balance between osmotic pressure driving the swelling and the gel elasticity, which generally opposes the swelling.[37] Swelling is high when the polymer is highly soluble in a given solvent and the cross-link density is relatively low.[38] While bulk gels swell isotropically in all three directions, surface-anchored gels swell anisotropically and exclusively in the direction perpendicular to the anchoring substrate.[39,40]

From the data in Figure 4 it is apparent that a gel with a given gel fraction swells more in methanol than in water. While water molecules can coordinate with the NIPAAm units via

hydrogen bonding, methanol swells the polymer repeat units much more, being more hydrophobic than water. Thermodynamically, methanol is a good solvent for NIPAAm ($\chi_{NIPAAm/methanol} < 0.46$)[41] while water is nearly a theta solvent for NIPAAm ($\chi_{NIPAAm/water} \sim 0.5$).[42] To further underline the role of polymer/solvent interactions (χ) in gel swelling, we examined swelling of the gels in *n*-hexanes, which are poor solvents for PNIPAAm.[41] As documented by data in Figure S6, exposing the gels to *n*-hexanes does not cause swelling of the gels.

Figure 5 presents the dependence of the swelling factor α for MABP/MABP gradients gels prepared from samples having two different initial thicknesses (blue solid (129 nm) and open (50 nm) squares). The α plotted as a function of the gel fraction are consistent between the two data sets. The fact that the values of α for a given gel fraction are identical among all gels and thicknesses studied reveals that the cross-link density within each gel of a given gel fraction is approximately the same regardless of their method of preparation. We further compared the values of solvent volume fraction (ϕ_1) determined from the effective medium approximation (EMA) approach against those calculated from the swelling factor in Figure S7. This excellent agreement between the two values of ϕ_1 indicates that the gels prepared by the various cross-linking approaches are uniform across their thickness because the ellipsometry data can be modeled by assuming that the gels form only a single homogeneous layer containing polymer and solvent.

In summary, we developed a simple and robust chemical approach to generate orthogonal gradient networks using two chemically independent cross-linkers (thermally and photoactivated) attached chemically to flat impenetrable supports. This method enables us to achieve complete control over the network properties by varying spatially the cross-link density of the coatings on a single specimen in a tunable and controllable manner. The network cross-link density plays a pivotal role in determining the extent of swelling as well as the modulus of the gel. The degree of swelling decreases with increasing the extent of cross-linking and vice versa. This work demonstrates a new synthetic route to prepare surface-attached orthogonal gradient networks that are useful in the design of suitable candidates for various biological applications. Detailed investigation of these gradient gels with the interaction of protein and cells will be presented in a subsequent paper.

EXPERIMENTAL SECTION

Materials

N-Isopropylacrylamide (NIPAm), chlorodimethylsilane, methylmethacryloyl chloride, allyl bromide, 4-hydroxybenzophenonone, Pd/C, and magnesium sulfate were purchased from Sigma-Aldrich, USA, and were used without further purification. 1,4-Dioxane, diethyl ether, toluene, tetrahydrofuran (THF), petroleum ether, *n*-hexane, 1-butanol, 2-propanol, methanol, and acetone were purchased from Fisher-Scientific, USA. Water used for swelling experiment was from Milli-Q-purification system with the product resistivity of 10–15 MΩ·cm (Millipore, Boston, MA). Silicon wafers (orientation [100], thickness 0.5 mm, and diameter 100 mm) were purchased from Silicon Valley Microelectronics.

Instrumentation

Film thicknesses were assessed using variable angle spectroscopic ellipsometry (VASE, J.A. Woollam, USA). Thermal cross-linking was produced using FP82HT Hot stage with FP90 Central Processor (Mettler Toledo, USA). Photo-cross-linking reactions were performed using Omnicure series-1000 UV lamp at the wavelength of 360 nm (Lumen Dynamics, USA). The intensity of UV light was measured employing ILT-1400-A radiometer–photometer (International Light Technology, USA). In all experiments, the UV lamp was allowed to warm for about 20–30 min prior to the cross-linking reactions for better reproducibility (cf. Figure S7). Dip-coater (KSV-NIMA, USA) was used to move the sample under the UV light for making photogradient surfaces. The polymer film was deposited using spin coater (PNM32 model, Headway Research, Inc., USA). The molecular weight of the polymer was determined using size exclusion chromatography (SEC, Wyatt Optilab rex detector along with Alliance waters 2695 separation module, USA). Functionality of the monomer and polymer was examined using 300 MHz ^{1}H NMR and ^{13}C NMR (Varian, USA).

Synthesis of Cross-Linkers and Polymers

Styrenesulfonyl Chloride (SSCl)—SSCl was synthesized in two steps following the procedure reported elsewhere.[29] 50 mL of thionyl chloride ($SOCl_2$) and 0.3 g of 2,6-di-*tert*-butyl-4-methylphenol in 60 mL of dry DMF were stirred in an ice bath; with that 20 g of 4-vinylbenzene acid of sodium salt was added in small portions for about 5–10 min. The reaction mixture was stirred for ~3 h until the mixture turned into a homogeneous solution. This solution was then allowed to stand in refrigerator overnight. The cold solution was slowly poured into 300 mL of ice water and then extracted twice with 100 mL of benzene. The extract was washed twice with 100 mL of cold water and dried over anhydrous $MgSO_4$, and the solvent was removed on a rotary evaporator at 35 °C. A pale yellow liquid was obtained, which was used immediately without further purification.

Styrene Sulfonyl Azide (SSAz)—2.27 g of styrenesulfonyl chloride (11.2 mmol, 1.00 equiv) was dissolved in 35 mL of acetone, and then an aliquot volume of water (35 mL) was added. The turbid reaction mixture was cooled to 0 °C, and 0.802 g of NaN_3 (12.33 mmol, 1.10 equiv) was added in small portions. After the reaction mixture was stirred for 1.5 h at 0 °C, the acetone was removed in vacuum (30 °C, 150 mbar), and the aqueous layer was extracted with diethyl ether (3 × 20 mL). The combined organic layers were dried over $MgSO_4$, and the solvent was evaporated at 30 °C. The resulting oil (2.19 g, 10.5 mmol, 94%) was dried in a vacuum and used in the polymerization reactions without further purification. ^{1}H NMR (300 MHz, $CDCl_3$), δ (ppm): 7.91 (d, 2H, C–H_{aro}), 7.61 (d, 2H, C–H_{aro}), 6.78 (dd, 1H, –CH═CH_2), 5.95 (d,1H, –CH═CHH_{cis}), 5.52 (d, 1H, –CH═CHH_{trans}). FTIR (neat): 3092, 3069, 2348, 2129, 1593, 1491, 1398, 1372, 1167, 1089, 990, 928, 846, 748, 657, 591, 555 cm^{-1}.

Methacryloyloxybenzophenone (MABP)—5.25 g of methacryloyl chloride in 20 mL of dichlormethane was added to the solution of 5.06 g of 4-hydroxybenzophenone in 100 mL of dichloromethane at 0 °C. The mixture was allowed to reach room temperature and stirred for ~16 h. After completion of the reaction, the mixture was filtered and the organic

phase was washed three times with 5% solution of HCl, 5% solution of $NaHCO_3$, and finally with water. The resulting solvent was dried over $MgSO_4$ and added to 200 mL of cold *n*-hexane and allowed to precipitate at −20 °C overnight. The monomer was subsequently filtered and recrystallized using ethyl acetate–hexane mixture. ^{1}H NMR (300 MHz, $CDCl_3$): δ = 2.1 ppm (s, 3H, *CH_3), δ = 5.7–6.3 ppm (2s, 2H, *CH_2═), δ = 7.1–7.9 ppm (various m, 9H, *C–H_{aro}). FT-IR: 3049 (═C–H), 2980–2927 (–C–H), 1732 (–C═O), 1653 (–HN–C═O), 1596 (–C═C–), and 1446 cm^{-1} (–C–H).

4-[3-(Triethoxysilyl)propyloxy]benzophenone (TESPBP)—5 g of 4-allyloxybenzophenone was dissolved in ~20 mL of freshly distilled dimethylchlorosilane. 70 mg of Pt–C was then added to the reaction mixture slowly, which was then refluxed at 120 °C for 5 h under nitrogen. After completion of the reaction, the excess triethoxysilane was removed by evaporation under vacuum. The catalyst was removed by filtration of the solution under nitrogen. This solution was then directly used to prepare the surface attached polymer networks. ^{1}H NMR (300 MHz, $CDCl_3$): δ = 0.8 ppm (t, 2H, CH_2–*CH_2–Si), δ = 1.2 ppm (m, 9H, *CH_3–CH_2–O), δ = 1.9 ppm (p, 2H, O–CH_2–*CH_2–CH_2–Si), δ = 3.8 ppm (q, 6H, CH_3-*CH_2–O), δ = 4.0 ppm (t, 2H, O–*CH_2–BP), δ = 7.8–6.9 ppm (m, 9H, C–H_{aro}).

Poly(NIPAm-co-5% MABP-co-5% SSAz)—The copolymer was synthesized through free-radical polymerization using AIBN as a free radical initiator. In a typical run, calculated amounts of PNIPAm (4.0776 g), MABP (0.522 g), SSAz (0.4184 g), and AIBN (0.00656 g) were dissolved in 10 mL of 1,4-dioxane and degassed under argon air by three freeze–thaw cycles. The mixture was placed in a preheated oil bath (60 °C) for ~16 h. The polymer was precipitated in petroleum ether and washed thoroughly with petroleum ether using 100 mL (100 × 4). We used exclusion chromatography (SEC) to determine the molecular weight distribution. The number-average molecular weight and polydispersity index were 339 kDa (PS standard) and 2.5, respectively.

Preparation Gradient Networks

A UVO-cleaned silicon wafer or glass substrate was used for the silanization. 4-[3-(Triethoxysilyl)propyloxy]benzophenone (TESPBP) (30 mmol) was freshly prepared in toluene and spin-cast onto the cleaned substrate at 1000 rpm for 60 s. The sample was then covered with aluminum foil and annealed at 120 °C overnight followed by extraction in toluene and drying over N_2 gas. This procedure yielded a monolayer of TESPBP (thickness 4–6 nm) on the silicon/glass substrate. The solution of precursor polymer was prepared with the concentration of 30 mg/mL in 1-butanol and filtered using a 0.45 μm filter. 100 μL of the solution was spin-coated onto a TESPBP-coated substrate at 2500 rpm for 60 s.

After evaporation of solvent, the polymer-coated wafer was placed on top of a gradient heating stage and cross-linked for 5 h. The horizontal gradient in temperature was obtained by heating the sample at one end and other end of the sample was rested to room temperature on closed chamber. This gives a temperature gradient across the sample varying from 140 to 25 °C. Subsequently, the sample was illuminated with UV light by moving the sample under the UV source at the speed of 10 mm/min for 4 min with a total dosage of 2

J/cm^2 as shown in Figure 1b. After photo-cross-linking, the sample was extracted with 1-butanol (overnight) to remove any unreacted polymer from the substrate surface. The film thickness of the deposited layer was measured using VASE.

Spectroscopic Ellipsometry

The thickness of the polymer films was determined by using variable angle spectroscopic ellipsometry (J.A. Woollam, USA). Reflectivity scans were collected at a 70° angle of incidence (relative to the vertical direction) in the spectral range of 400–1000 nm in 60 steps (10 nm/step) for 3 min. Measurements were made on the UVO-cleaned silicon wafer deposited with polymer, after cross-linking and after washing the samples. For gradient surfaces, the sample was divided into 3 × 3 matrices (squares) with 1 × 1 cm^2 dimensions, and 2–3 measurements were collected on each square. The ellipsometry data were modeled based on Fresnel formulizm using a three-layer model in WVASE32 software (J.A. Woollam Co., version 3.682): (1) Si, (2) SiO_2, (3) polymer adlayer (Cauchy function, $A_n = 1.5$, $B_n = 0.01$, $k = 0$).

Swelling measurements were performed using the liquid cell adopted with VASE. The cell is filled with ~200 mL of solvent (water or methanol), and the sample was immersed in the solvent, allowed to reach equilibrium for ~5–10 min. We validated that these times were sufficient to reach an equilibrium swelling in thin network films. The thickness of swollen network did not change after ~2 min of exposure to a solvent. The reflectivity scans from swollen gels were recorded at a 70° angle of incidence from 400 to 1000 nm spectral range in 60 steps (10 nm/step) for 3 min. The swollen thickness and volume fraction of the gel were determined based on effective medium approximation (EMA) method (cf. Figure S7). The reflectivity scans were collected to deduce the swelling of a polymer film. For humidity swelling, a custom-made PMMA lid with single opening was utilized to access the relative humidity–temperature sensor (Omega Engineering). The sensor was connected to computer via USB, and the change in RH was monitored. The relative humidity of the environment was controlled using saturated salt solution of K_2SO_4 and KOH containing vial caps placed inside the liquid cell.

Supplementary Material

Refer to Web version on PubMed Central for supplementary material.

ACKNOWLEDGMENTS

This work was supported by the Office of Naval Research under Grant N000141210642 (J.G.). M.R. acknowledges financial support from the National Science Foundation under Grants DMR-1309892, DMR-1436201, the National Institutes of Health under Grants P01-HL108808 and 1UH2HL123645, and the Cystic Fibrosis Foundation. This work was also supported in part by the NSF's Research Triangle MRSEC (DMR-1121107).

REFERENCES

(1). Genzer, J. Soft Matter Gradient Surfaces - Methods and Applications. John Wiley & Sons; New York: 2012.

(2). Sant S, Hancock MJ, Donnelly JP, Iyer D, Khademhosseini A. Biomimetic gradient hydrogels for tissue engineering. Can. J. Chem. Eng. 2010; 88:899–911. [PubMed: 21874065]

(3). Dertinger SKW, Jiang XY, Li ZY, Murthy VN, Whitesides GM. Gradients of substrate-bound laminin orient axonal specification of neurons. Proc. Natl. Acad. Sci. U. S. A. 2002; 99:12542–12547. [PubMed: 12237407]

(4). Wang Q, Bohn PW. Active spatiotemporal control of Arg-Gly-Asp-containing tetradecapeptide organomercaptans on gold with in-plane electrochemical potential gradients. J. Phys. Chem. B. 2003; 107:12578–12584.

(5). Ionov L, Houbenov N, Sidorenko A, Stamm M, Minko S. Smart microfluidic channels. Adv. Funct. Mater. 2006; 16:1153–1160.

(6). Wegst UGK, Bai H, Saiz E, Tomsia AP, Ritchie RO. Bioinspired structural materials. Nat. Mater. 2015; 14:23–36. [PubMed: 25344782]

(7). Kim TH, An DB, Oh SH, Kang MK, Song HH. Creating stiffness gradient polyvinyl alcohol hydrogel using a simple gradual freezing-thawing method to investigate stem cell differentiation behaviors. Biomaterials. 2014; 40:51–60. [PubMed: 25467820]

(8). Chaudhury MK, Whitesides GM. How to make water run uphill. Science. 1992; 256:1539–1541. [PubMed: 17836321]

(9). Ichimura K, Oh SK, Nakagawa M. Light-driven motion of liquids on a photoresponsive surface. Science. 2000; 288:1624–1626. [PubMed: 10834837]

(10). Baier H, Bonhoeffer F. Axon guidance by gradients of a target-derived component. Science. 1992; 255:472–475. [PubMed: 1734526]

(11). Kloxin AM, Benton JA, Anseth KS. In situ elasticity modulation with dynamic substrates to direct cell phenotype. Biomaterials. 2010; 31:1–8. [PubMed: 19788947]

(12). Kloxin AM, Tibbitt MW, Kasko AM, Fairbairn JA, Anseth KS. Tunable hydrogels for external manipulation of cellular microenvironments through controlled photodegradation. Adv. Mater. 2010; 22:61–66. [PubMed: 20217698]

(13). Genzer J. Surface-bound gradients for Studies of soft materials behavior. Annu. Rev. Mater. Res. 2012; 42:435–468.

(14). Genzer J, Bhat RR. Surface-bound soft matter gradients. Langmuir. 2008; 24:2294–2317. [PubMed: 18220435]

(15). Genzer J, Arifuzzaman S, Bhat RR, Efimenko K, Ren C, Szleifer I. Time dependence of lysozyme adsorption on end-grafted polymer layers of variable grafting density and length. Langmuir. 2012; 28:2122–2130. [PubMed: 22181708]

(16). Crowe-Willoughby JA, Weiger KL, Ozcam AE, Genzer J. Formation of silicone elastomer networks films with gradients in modulus. Polymer. 2010; 51:763–773.

(17). Jhon YK, Semler JJ, Genzer J, Beevers M, Guskova O, Khalatur P, Khokhlov AR. Effect of comonomer sequence distribution on the adsorption of random copolymers onto impenetrable flat surfaces. Macromolecules. 2009; 42:2843–2853.

(18). Seidi A, Ramalingam M, Elloumi-Hannachi I, Ostrovidov S, Khademhosseini A. Gradient biomaterials for soft-to-hard interface tissue engineering. Acta Biomater. 2011; 7:1441–1451. [PubMed: 21232635]

(19). Ionov L, Zdyrko B, Sidorenko A, Minko S, Klep V. Gradient polymer layers by “grafting to” approach. Macromol. Rapid Commun. 2004; 25:360–365.

(20). Ionov L, Sidorenko A, Stamm M, Minko S, Zdyrko B. Gradient mixed brushes: “Grafting to” approach. Macromolecules. 2004; 37:7421–7423.

(21). Bhat RR, Tomlinson MR, Genzer J. Assembly of nanoparticles using surface-grafted orthogonal polymer gradients. Macromol. Rapid Commun. 2004; 25:270–274.

(22). Morgenthaler S, Zink Ch. Spencer N. Surface-chemical and -morphological gradients. Soft Matter. 2008; 4:419–434.

(23). Fuierer RR, Carroll L, Feldheim DL, Gorman CB. Patterning mesoscale gradient structures with self-assembled monolayers and scanning lithography. Adv. Mater. 2002; 14:154–157.

(24). Schuh C, Santer S, Prucker O, Rühe J. Polymer brushes with nanometer-scale gradients. Adv. Mater. 2009; 21:4706–4710.

(25). Daniel S, Chaudhury MK, Chen JC. Fast drop movements resulting from the phase change on a gradient surface. Science. 2001; 291:633–636. [PubMed: 11158672]

(26). Wang L, Peng B, Su Z. Tunable wettability and rewritable wettability gradient from superhydrophilicity to superhydrophobicity. Langmuir. 2010; 26:12203–12208. [PubMed: 20415506]

(27). Geisen U, Heilmann C, Beyersdorf F, Benk C, Herz U, Schlensak U, Budde U, Zieger B. Non-surgical bleeding in patients with ventricular assist devices could be explained by acquired von Willebrand disease. Eur. J. Cardiothorac. Surg. 2008; 33:679–684. [PubMed: 18282712]

(28). Pandiyarajan CK, Prucker O, Zieger B, Rühe J. Influence of the molecular structure of surface-attached poly(N-alkyl acrylamide) coatings on the interaction of surfaces with proteins, cells and blood platelets. Macromol. Biosci. 2013; 13:873–884. [PubMed: 23596084]

(29). Ionov L, Houbenov N, Sidorenko A, Stamm M, Minko S. Smart microfluidic channels. Adv. Funct. Mater. 2006; 16:1153–1160.

(30). Schuh K, Prucker O, Rühe J. Surface attached polymer networks through thermally induced cross-linking of sulfonyl azide group containing polymers. Macromolecules. 2008; 41:9284–9289.

(31). Ortiz O, Vidyasagar A, Wang J, Toomey R. Surface instabilities in ultrathin, cross-linked poly(N-isopropylacrylamide) coatings. Langmuir. 2010; 26:17489–17494. [PubMed: 20929198]

(32). Vidyasagar A, Majewski J, Toomey R. Temperature Induced Volume-Phase Transitions in Surface-Tethered Poly(N -isopropylacrylamide) Networks. Macromolecules. 2008; 41:919–924.

(33). DuPont SJ Jr. Cates RS, Stroot PG, Toomey R. Swelling-induced instabilities in microscale, surface-confined poly(N-isopropylacryamide) hydrogels. Soft Matter. 2010; 6:3876–3882.

(34). Prucker O, Naumann CA, Rühe J, Knoll W, Frank CW. Photochemical attachment of polymer films to solid surfaces via monolayers of benzophenone derivatives. J. Am. Chem. Soc. 1999; 121:8766–8770.

(35). Pandiyarajan, CK. The Interaction of Blood Proteins and Platelets on Surface-Attached Poly(alkylacrylamide) Networks. Der Andere Verlag; Germany: 2013.

(36). Panyukov, S.; Pandiyarajan, CK.; Genzer, J.; Rubinstein, M. Manuscript in preparation.

(37). Flory PJ, Rehner J. Statistical mechanics of cross-linked polymer networks I. Rubberlike elasticity. J. Chem. Phys. 1943; 11:512–520.

(38). Flory PJ. Statistical mechanics of cross-linked polymer networks II. Swelling. J. Chem. Phys. 1943; 11:521–526.

(39). Toomey R, Freidank D, Rühe J. Swelling behavior of thin, surface-attached polymer networks. Macromolecules. 2004; 37:882–887.

(40). Rubinstein, M.; Colby, RH. Polymer Physics. Oxford University Press; 2003.

(41). Zhang G, Wu C. The water/methanol complexation induced reentrant coil-to-globule-to-coil transition of individual homopolymer chains in extremely dilute solution. J. Am. Chem. Soc. 2001; 123:1376–1380.

(42). Pandiyarajan, CK.; Lorchat, P.; Genzer, J.; Rubinstein, M. Unpublished data

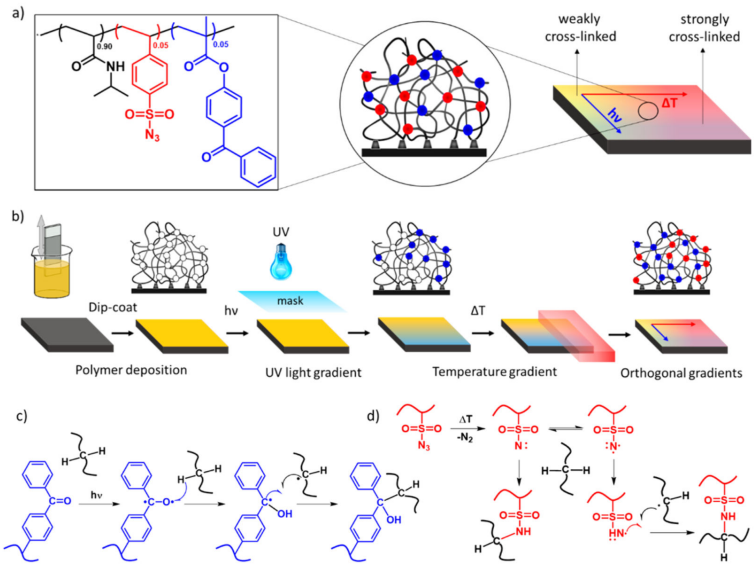

Figure 1.

(a) Schematic diagram of an orthogonal gradient network comprising poly(NIPAAm$_{0.90}$-*co*-SSAz$_{0.05}$-*co*-MABP$_{0.05}$). (b) Preparation of orthogonal gradient networks where the base polymer was deposited on a silicon or glass substrate via spin-coating. The sample was moved under a UV lamp horizontally at a speed of 10 mm/min, which led to photo-cross-linking with a gradient in UV dosage. Next, the sample was placed on top of a gradient heating stage (orthogonally to the UV cross-linking direction) to achieve a gradient in thermally activated cross-links. After cross-linking, the sample was extracted with solvent to remove any polymeric material that was not connected to the network. The sample was dried, and the film thickness and corresponding gel fraction were determined using variable angle spectroscopic ellipsomtery (VASE). (c, d) Cross-linking mechanisms of the photo (blue) and thermal (red) cross-linkers.

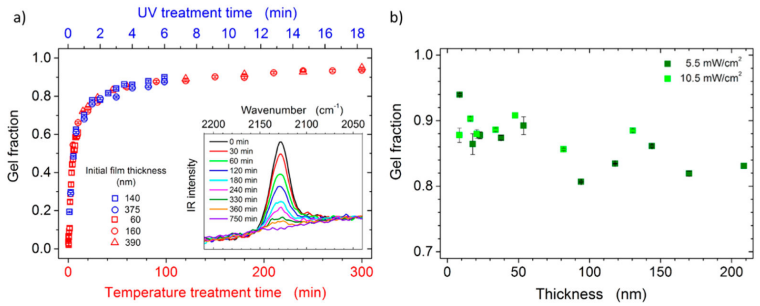

Figure 2.

Kinetics of the gel formation of poly(NIPAAm$_{0.90}$-*co*-SSAz$_{0.05}$-*co*-MABP$_{0.05}$). (a) Gel fraction in the photo-cross-linking (blue data) and thermal cross-linking (red data) processes as a function of treatment time (UV exposure time is denoted by the upper abscissa in blue and temperature exposure time is depicted by the lower abscissa in red). The various symbols represent initial thicknesses of the copolymer films before UV/thermal treatment. The inset shows FT-IR spectra collected from thermally cross-linked samples for various treatment times. (b) Gel fraction as a function of the initial film thickness for two different UV dosages identified in the legend.

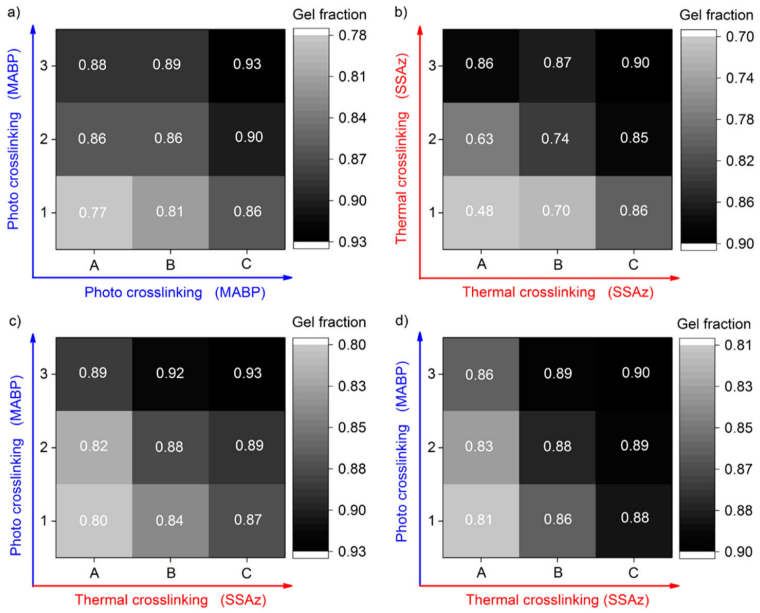

Figure 3.

Gel fraction of surface-attached orthogonal gradient networks comprising poly(NIPAAm$_{0.90}$-*co*-SSAz$_{0.05}$-*co*-MABP$_{0.05}$) on TESPBP-covered silicon wafer (a: MABP/MABP; b: SSAz/SSAz; c: MABP/SSAz) and (d) MABP/SSAz on PMMA-covered surface. The samples are labeled in an ascending order so that A and 1 are low in thickness or C and 3 are high in thickness. Dark region of the graphs and the corresponding numbers indicate the higher gel content/film thickness. The actual photographs of the samples are presented in Figure S2.

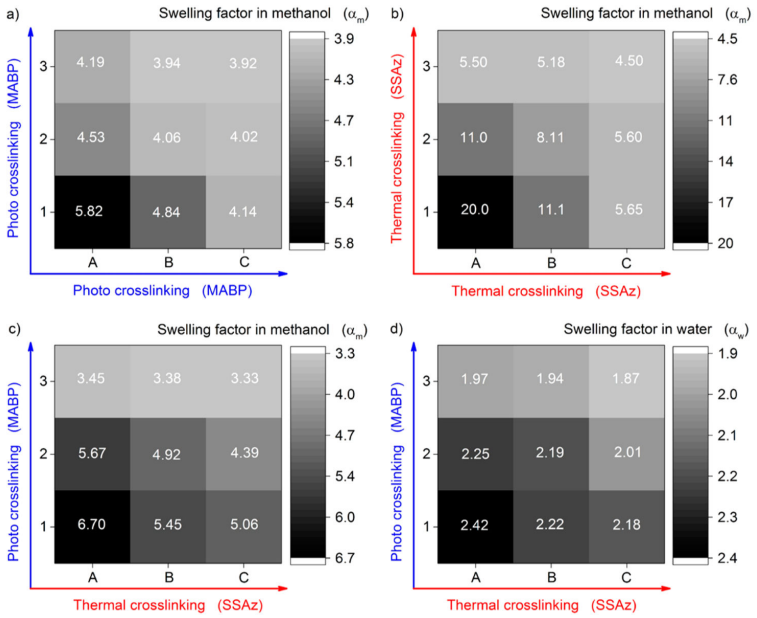

Figure 4.

Swelling factor (α) of surface-attached MABP/MABP, SSAz/SSAz, and MAPB/SSAz orthogonal gradient network (prepared by thermal and UV cross-linking) in methanol (a–c) and water (d).

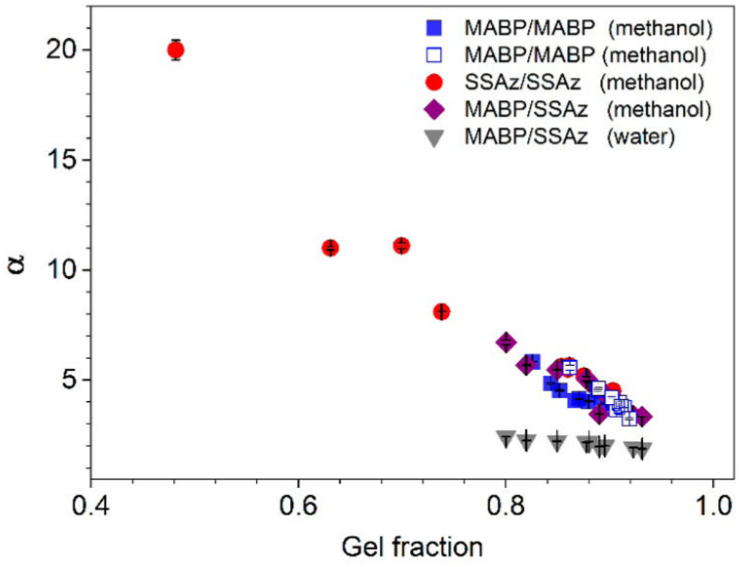

Figure 5.

Swelling factor of surface-attached poly(NIPAAm$_{0.90}$-*co*-SSAz$_{0.05}$-*co*-MABP$_{0.05}$) orthogonal network as a function of gel fraction. The solid and open symbols for MABP/MABP correspond to samples with an initial dry thickness (before cross-linking) of 129 and 50 nm, respectively.